

- [7] J. F. Diaz, K. J. Balkus, Jr, F. Bedioui, V. Kurshev, L. Kevan, *Chem. Mater.* **1997**, *9*, 61.
- [8] F. A. Cotton, G. Wilkinson, *Advanced Inorganic Chemistry*, Wiley, New York, **1988**.
- [9] a) S. Dai, Y. S. Shin, C. E. Barnes, L. M. Toth, *Chem. Mater.* **1997**, *9*, 2521; b) S. Dai, Y. S. Shin, C. E. Barnes, L. M. Toth, *J. Phys. Chem. B* **1997**, *101*, 5521.
- [10] See for example a) G. Wulff, *Angew. Chem.* **1995**, *107*, 1958; *Angew. Chem. Int. Ed. Engl.* **1995**, *34*, 1812; b) K. J. Shea, *Trends Polym. Sci.* **1994**, *2*, 166; c) K. Mosbach, *Trends Biochem. Sci.* **1994**, *19*, 9; d) J. Steinke, D. C. Sherrington, I. R. Dunkin, *Adv. Polym. Sci.* **1995**, *123*, 81; e) P. A. Brady, J. M. Sanders, *Chem. Soc. Rev.* **1997**, *26*, 327; f) *Molecular and Ionic Recognition with Imprinted Polymers*, (Eds.: R. A. Bartsch, M. Maeda), ACS, Washington, DC, **1998**.
- [11] W. Kuchen, J. Schram, *Angew. Chem.* **1988**, *100*, 1757; *Angew. Chem. Int. Ed. Engl.* **1988**, *27*, 1695.
- [12] Surface imprinting of inorganic and organic molecules on amorphous flat silica surfaces and organic polymer surfaces have been conducted previously, see a) G. Wulff, B. Heide, G. Helfmeier, *J. Am. Chem. Soc.* **1986**, *108*, 1089; b) K. J. Shea, T. K. Dougherty, *J. Am. Chem. Soc.* **1986**, *108*, 1091; c) K. Y. Yu, K. Tsukagoshi, M. Maeda, M. Takagi, *Anal. Sci.* **1992**, *8*, 701.
- [13] Small angle X-ray scattering of the mesoporous samples was measured at the SAXS User Facility of the Oak Ridge National Laboratory.
- [14] E. P. Barrett, L. G. Joyner, P. B. Halenda, *J. Am. Chem. Soc.* **1951**, *73*, 373.
- [15] a) K. Tsukagoshi, K. Y. Yu, M. Maeda, M. Takagi, *Bull. Chem. Soc. Jpn.* **1993**, *66*, 114; b) K. Tsukagoshi, K. Y. Yu, M. Maeda, M. Takagi, T. Miyajima, *Bull. Chem. Soc. Jpn.* **1995**, *68*, 3095; c) V. A. Kabanov, A. A. Efendiev, D. D. Orujev, *J. Appl. Polym. Sci.* **1979**, *24*, 259; d) H. Nishide, J. Deguchi, E. Tsuchida, *J. Polym. Sci.* **1977**, *15*, 3023.
- [16] a) A. M. Klonowski, C. W. Schlaepfer, *J. Non-Cryst. Solids* **1991**, *129*, 101; b) G. De, M. Epifani, A. Licculli, *J. Non-Cryst. Solids* **1996**, *201*, 250.
- [17] A version of Allinger's MMP2 program by J. J. Gajewski and K. E. Gilbert. This program is available from Serena Software, P.O. Box 3076, Bloomington, IN 47402–3076 (USA).
- [18] Methanol was chosen as the solvent in which to conduct the imprint coating of  $[\text{Cu}(\text{aapts})_2\text{S}_2]^{2+}$ , while water was used as the solvent for the imprint coating of  $[\text{Cu}(\text{aapts})_2\text{S}_{6-1}]^{2+}$ . The reason for choosing water to imprint the latter is that the stability constant of  $\text{Cu}^{2+}$  complexed to APTS is very small in methanol. For the procedure of coating in methanol solution, see H. Ince, S. Akman, U. Koklu, *Fresenius J. Anal. Chem.* **1992**, *342*, 560. For the procedure of coating in water solution, see C. H. Chiang, H. Ishida, J. Koenig, *J. Colloid Inter. Sci.* **1980**, *74*, 396.
- [19] A. B. P. Lever, *Inorganic Electronic Spectroscopy*, Elsevier, New York, **1968**.
- [20] A. Baker, *J. Chem. Edu.* **1998**, *75*, 98.
- [21] a) G. S. Carajal, D. E. Leyden, G. R. Quiting, G. E. Maciel, *Anal. Chem.* **1988**, *60*, 1776; b) A. Yoshino, H. Okabayashi, I. Shimizu, C. J. O'Connor, *Colloid Polym. Sci.* **1997**, *275*, 672.
- [22] *Pure Appl. Chem.* **1972**, *29*, 619.
- [23] The highest enhancement of  $K_d$  for  $\text{Cu}^{2+}$  through imprint coating on commercial, amorphous silica is 1.54, which is much less than the best value obtained on the ordered mesopore surfaces.
- [24] We have also developed sorbents coated with the imprints of  $[\text{Zn}(\text{aapts})_2]^{2+}$  and  $[\text{Hg}(\text{aapts})_2]^{2+}$  for the selective adsorption of  $\text{Zn}^{2+}$  and  $\text{Hg}^{2+}$ . The adsorption capacities of both sorbents were increased by surface imprinting. In the case of the  $\text{Zn}^{2+}$ -imprinted sorbent a 100% adsorption of  $\text{Zn}^{2+}$  in 10 mL of a  $10^{-3}\text{M}$  solution by 0.1 g of the sorbent was observed. The selectivity of the sorbent imprinted with  $[\text{Zn}(\text{aapts})_2]^{2+}$  was tested using the  $\text{Zn}^{2+}/\text{Cu}^{2+}$  system. The value of  $k'$  is 3.3.

## Strong N–H...O Hydrogen Bonding in a Model Compound of the Catalytic Triad in Serine Proteases\*\*

Jacob Overgaard, Birgit Schiøtt, Finn K. Larsen, Arthur J. Schultz, John C. MacDonald, Bo B. Iversen\*

The cleavage of peptide bonds is an important reaction in nature that involves the catalytic triad of residues (Ser-His-Asp) in the active site of the serine proteases class of enzymes (Figure 1).<sup>[1]</sup> A number of studies have suggested that a low-barrier hydrogen bond (LBHB) is involved in the reaction

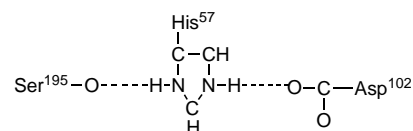


Figure 1. Schematic drawing of the catalytic triad in serine proteases. No formal charges or bond orders have been assumed in the sketch.

mechanism as a partial proton transfer between His<sup>57</sup> and Asp<sup>102</sup>.<sup>[2]</sup> Formation of a LBHB can account for many of the special physicochemical observations found in some enzymes, but it is still a matter of controversy whether a LBHB contributes significantly toward the catalytic activity of the triad.<sup>[3]</sup> Much research has been carried out to examine the nature of short, strong hydrogen bonds, and the principal tools of analysis have been ab initio computations on small model systems,<sup>[4]</sup> crystal structure correlations,<sup>[5]</sup> and spectroscopic investigations.<sup>[6]</sup> It is increasingly evident that a number of factors besides the distance between heteroatoms influences the formation of a LBHB. Factors such as matching of  $pK_a$  values, involvement in other hydrogen bonds, and steric strain are also of importance. Analysis of charge densities (CDs) in model systems provides an alternative method for studying hydrogen bonds. Charge densities in hydrogen bond systems can be determined experimentally from combined analysis of low-temperature X-ray and neutron diffraction data.<sup>[7]</sup> Contrary to ab initio theory, experimental CD studies have far fewer restrictions on the size of the model system that can be studied, and the results inherently reflect all interactions in the crystal. Detailed quantitative information about the

[\*] Dr. B. B. Iversen, J. Overgaard, B. Schiøtt, F. K. Larsen  
Department of Chemistry, University of Aarhus  
DK-8000 Aarhus (Denmark)  
Fax: (+45)86196199  
E-mail: bo@kemi.aau.dk

Dr. A. J. Schultz  
Intense Pulsed Neutron Source, Argonne National Laboratory  
Argonne, IL 60439 (USA)

Dr. J. Macdonald  
Department of Chemistry, Northern Arizona University, Flagstaff,  
AZ-86011 (USA)

[\*\*] Work at Argonne was supported by the U.S. Department of Energy, BES-Materials Science, under contract No. W-31-109-ENG-38. The SUNY X3 beamline at NSLS is supported by the Division of Basic Energy Sciences of the U.S. Department of Energy (DE-FG02-86ER45231). The synchrotron work is supported by the DANSYNC grant from the Danish Research Councils.

bonding can be obtained by Bader topological analysis of the CD.<sup>[8]</sup>

In order to investigate the electronic structure of short N–H...O bonds, we have carried out combined low-temperature (28(1) K) X-ray and neutron diffraction studies of the cocrystal between betaine, imidazole, and picric acid (Figure 2). The complex serves as a model for the catalytic triad,

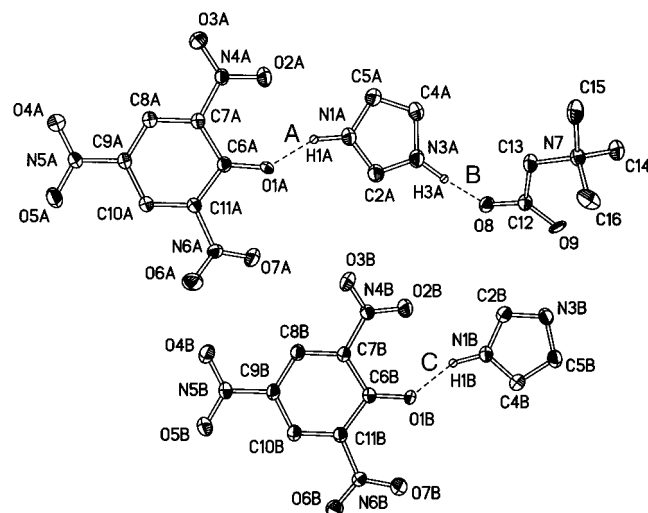


Figure 2. Cocrystal of betaine, imidazole, and picric acid (ORTEP drawing at 95% probability level based on neutron diffraction data at 28 K). Hydrogen atoms have been omitted for clarity. A short C–H...O interaction exists between C8B–H8B...O7A (3.070(3) Å), which is important for the crystal packing.

and the system is attractive a priori since it contains three different short N–H...O contacts (<2.7 Å) in the same crystal. This enables us to investigate factors such as matching of  $pK_a$  values and three center hydrogen bonding without the effects of differences in systematic errors between different experiments normally encountered in crystal structure correlations.

To achieve high resolution within strict neutron beam time limitations we employed the white beam time-of-flight neutron diffraction technique at the SCD station at the Intense Pulsed Neutron Source.<sup>[9]</sup> The structure contains 75 unique atoms in the asymmetric unit making it one of the

largest structures investigated to high resolution ( $d_{\min} > 0.38$  Å) by neutron diffraction. High resolution is critical to define the thermal motion of the atoms properly. Refinement of anharmonic thermal parameters provides an experimental probe for the shape of the potential energy surface for proton transfer.<sup>[7]</sup> X-ray data at matching temperatures were collected on two different crystals using both synchrotron radiation and conventional sealed tube radiation. The synchrotron data were collected to high resolution at beam line X3A1 at the National Synchrotron Light Source using image plate detectors, but for technical reasons the data was not complete in the low-order region. Therefore, complete low-order data were collected on a four-circle sealed tube diffractometer. Since extinction in both crystals was negligible, the two data sets were refined simultaneously in the CD modeling.

None of the atoms showed significant anharmonic thermal parameters in the refinement against the neutron data. Furthermore the atomic mean square displacements are not conspicuous in size. This result indicates that the potential energy surfaces of all the hydrogen bonds in the complex consist of two separate harmonic potential wells. The structural parameters for the 25 hydrogen atoms derived from the neutron data were used at fixed values in the refinement against the X-ray data. The charge density was modeled with the Hansen–Coppens multipole model,<sup>[10]</sup> which accurately describes aspherical density distributions for compounds containing second row elements.

Bond lengths and topological properties for the three short hydrogen bonds are listed in Table 1. The neutron data reveal a significant lengthening of the N–H distances relative to weakly bonded systems (1.0 Å), and the lengthening fits well with the N–H versus H...O distance correlations established by Steiner.<sup>[5b]</sup> The data show that all the hydrogen atoms are localized at the nitrogen atoms, and that none are involved in LBHBs. The absence of LBHBs is supported by the topological analysis, which shows the O...H interactions to be predominantly electrostatic interactions ( $\nabla^2\rho > 0$ ) between closed-shell atoms (Figure 3). It is, however, clear that especially bond B has a considerable polarization of the Laplacian (Laplacian operator of the electron density function) towards the acceptor atom. Madsen et al. have shown that in LBHBs the fundamental nature of the interaction is

Table 1. Topological properties of the short, strong hydrogen bonds.  $\rho$  is the electron density and  $\nabla^2\rho$  the Laplacian at the bond critical points.  $q_1$  and  $q_2$  are atomic charges derived from the charge density.  $V$  and  $T$  are the potential energy density and the kinetic energy density, respectively.  $E_{\text{HB}}$  is the hydrogen bond energy.

Bond		$D_{\text{neutron}}$ [Å]	$\angle \text{N–H...O}$ [°]	$\rho$ [e Å <sup>-3</sup> ]	$\nabla^2\rho$ [e Å <sup>-5</sup> ]	$q_1$ <sup>[a]</sup>	$q_2$ <sup>[a]</sup>	$V$ <sup>[b]</sup> [kcal mol <sup>-1</sup> ]	$T$ <sup>[b]</sup> [kcal mol <sup>-1</sup> ]	$E_{\text{HB}} = -\frac{1}{2}V$ <sup>[c]</sup> [kcal mol <sup>-1</sup> ]
A	N1A–O1A	2.613(2)	154.5(5)							
	N1A–H1A	1.046(4)		2.00	–30.7	–0.04	0.23			
	H1A–O1A	1.631(4)		0.37	3.2	0.23	–0.20	–34.9 (–33.8) <sup>[d]</sup>	28.0 (33.5)	17.4 (16.9)
B	N3A–O8	2.685(2)	171.2(4)							
	N3A–H3A	1.056(4)		1.87	–29.9	–0.08	0.28			
	H3A–O8	1.637(4)		0.41	1.8	0.28	–0.38	–37.8 (–33.0)	24.8 (32.9)	18.9 (16.5)
C	N1B–O1B	2.676(2)	157.2(4)							
	N1B–H1B	1.049(4)		2.00	–34.6	–0.05	0.28			
	H1B–O1B	1.678(4)		0.30	3.0	0.28	–0.20	–26.2 (–28.4)	23.0 (29.4)	13.1 (14.2)

[a] Based on spherical kappa refinement. [b] Y. A. Abramov, *Acta Crystallogr. Sect. A* **1997**, 53, 264–272. [c] E. Espinosa, E. Molins, C. Lecomte, *Chem. Phys. Lett.* **1998**, 285, 170–173. [d] Values in parentheses are calculated based on correlations established in [c] for normal hydrogen bonds.

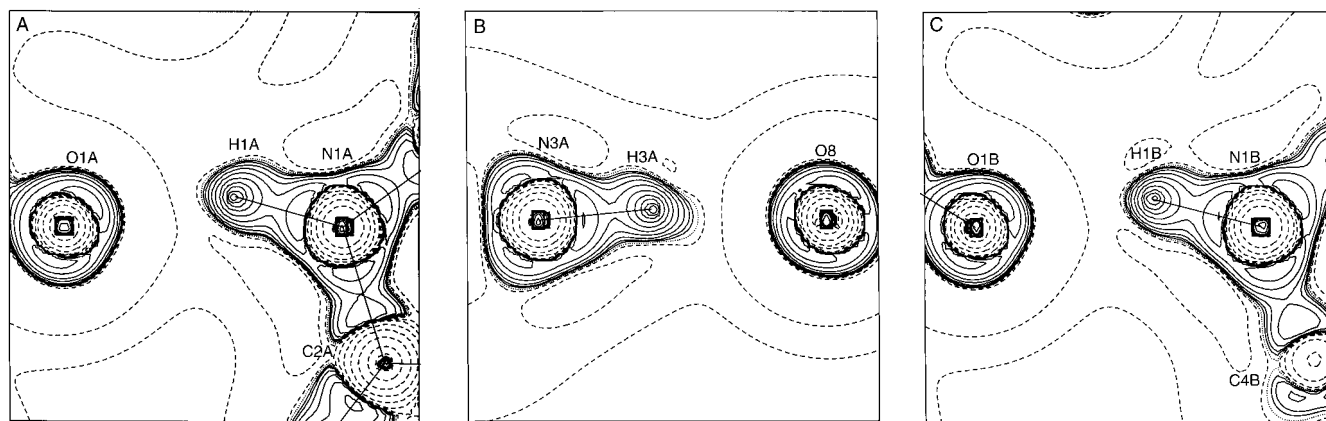


Figure 3. Contour plot of the negative of the Laplacian of the electron density in the planes of the three strong N–H...O hydrogen bonds. A) N1A–H1A...O1A; B) N3A–H3A...O8; C) N1B–H1B...O1B. The contours are drawn at logarithmic intervals of  $1.0 \times 2^N \text{ e } \text{\AA}^{-5}$ . The dotted line is the zero contour. Solid lines are positive contours, and broken lines are negative contours.

different than in longer hydrogen bonds, and the hydrogen atom becomes partly covalently bonded to both heteroatoms.<sup>[7]</sup>

If the heteroatom distance uniquely defines the nature of the hydrogen bonds, then the present study could be used to establish an upper limit for the distance of N–H...O LBHBs in enzymes (2.613(2) Å). There are, however, subtleties in the N–H...O bond properties that indicate other factors are important. For example, the N–H distance is marginally longer in bond B than in bond A, even though the N...O and O...H distances are longer in bond B (Figure 1, Table 1). Furthermore bond B is a two-center bond, whereas bonds A and C are three-center bonds with longer secondary hydrogen bond interactions (O2A...H1A 2.312(5) Å, O2B...H1B 2.242(5) Å). The secondary interactions will further lengthen the N–H distances in bonds A and C. The longer N–H distance in bond B may be due to a better  $pK_a$  match between betaine (1.8) and the imidazolium ion (7.0) than between the imidazolium ion and picric acid (0.4) ( $pK_a(\text{imidazole}) = 10.5$ ). The topological analysis reveals that the strongest hydrogen bond is formed in bond B, although all three hydrogen bonds are strong with bonding energies exceeding those of normal hydrogen bonds (2–10 kcal mol<sup>−1</sup>). In fact the bond energies ( $E_{\text{HB}}$ ) are very similar to the LBHB of benzoylacetone (16 kcal mol<sup>−1</sup>).<sup>[4c]</sup> This study demonstrates that short, strong hydrogen bonds do not have to be low-barrier. The estimate of the bond energy  $E_{\text{HB}}$  is, however, only strictly valid for electrostatic interactions; the present hydrogen bonds deviate from the correlations established previously for a large number of normal hydrogen bonds.<sup>[11]</sup> Our data therefore indicates that the strong hydrogen bonds in the present complex are not entirely electrostatic in character. The smaller positive value of  $\nabla^2\rho$  in bond B indicates that bond B has most covalency and thus is closest to being a LBHB system. Furthermore the atomic charges of bond B are larger than in the two other hydrogen bonds (Table 1), although still smaller than in the LBHB of benzoylacetone (O(−0.51(5)), H(+0.40(3)), O(−0.45(4))).<sup>[7]</sup> The transition to covalency appears to occur without abrupt changes in the character of the hydrogen bond interaction. It is notable that the bond that best mimics the His<sup>57</sup>–Asp<sup>102</sup> structure (bond B), also is closest to being a LBHB. It seems reasonable that to attain a

LBHB in bond B more charge needs to be added to N3A, and to a lesser extent removed from H3A. If low-barrier hydrogen bonds in fact are present in enzymes, then other factors not active in the present model complex must account for this charge migration. A possible explanation could be the electron-donating CH<sub>2</sub> groups present in histidine that are absent in imidazole. We are currently performing high-level ab initio calculations on our model system to gain further insights about the triad and to provide a detailed comparison with the experimental results.

#### Experimental Section

The cocrystal of C<sub>5</sub>N<sub>2</sub>O<sub>2</sub>H<sub>11</sub>, C<sub>3</sub>N<sub>2</sub>H<sub>5</sub>, and C<sub>6</sub>N<sub>3</sub>O<sub>7</sub>H<sub>2</sub> (C<sub>23</sub>N<sub>11</sub>O<sub>16</sub>H<sub>25</sub> in the asymmetric unit, FW = 711.51 g mol<sup>−1</sup>) belongs to the monoclinic space group *C2/c*. Crystallographic data (excluding structure factors) for the structure reported in this paper have been deposited with the Cambridge Crystallographic Data Center as supplementary publication no. CCDC-112286. Copies of the data can be obtained free of charge on application to CCDC, 12 Union Road, Cambridge CB21EZ, UK (fax: (+44) 1223-336-033; e-mail: deposit@ccdc.cam.ac.uk).

Neutron diffraction:  $T = 28(1) \text{ K}$ ,  $a = 33.536(5) \text{ \AA}$ ,  $b = 7.636(1) \text{ \AA}$ ,  $c = 25.066(4) \text{ \AA}$ ,  $\beta = 114.90(1)^\circ$ ,  $V = 5822(2) \text{ \AA}^3$ ,  $V_{\text{crystal}} = 13.2 \text{ mm}^3$ ,  $0.7 < \lambda < 4.2 \text{ \AA}$ , complete data out to  $(\sin\theta/\lambda)_{\text{max}} = 0.81 \text{ \AA}^{-1}$ , partial data out to  $(\sin\theta/\lambda)_{\text{max}} = 1.3 \text{ \AA}^{-1}$ ,  $\mu_a$  (true absorption at  $\lambda = 1.8 \text{ \AA}$ ) =  $1.22 \text{ cm}^{-1}$ ,  $\mu_s$  (total scattering) =  $1.15 \text{ cm}^{-1}$  (absorption correction performed), No. of measured reflections = 29014.

Synchrotron X-ray diffraction:  $T = 28(1) \text{ K}$ ,  $a = 33.54(2) \text{ \AA}$ ,  $b = 7.64(2) \text{ \AA}$ ,  $c = 24.98(4) \text{ \AA}$ ,  $\beta = 114.76(5)^\circ$ ,  $V = 5813(30) \text{ \AA}^3$ ,  $V_{\text{crystal}} = 0.001 \text{ mm}^3$ ,  $\lambda = 0.643(1) \text{ \AA}$ ,  $(\sin\theta/\lambda)_{\text{max}} = 1.08 \text{ \AA}^{-1}$ ,  $\mu_1 = 0.08 \text{ cm}^{-1}$  (no absorption correction), No. of measured reflections = 98 132, No. of unique = 15 657,  $R_{\text{int}} = 0.030$ .

Sealed tube X-ray diffraction:  $T = 10(1) \text{ K}$ ,  $a = 33.57(1) \text{ \AA}$ ,  $b = 7.640(2) \text{ \AA}$ ,  $c = 25.031(8) \text{ \AA}$ ,  $\beta = 114.84(2)^\circ$ ,  $V = 5826(6) \text{ \AA}^3$ ,  $V_{\text{crystal}} = 0.058 \text{ mm}^3$ ,  $\lambda = 0.5616 \text{ \AA}$ ,  $(\sin\theta/\lambda)_{\text{max}} = 0.51 \text{ \AA}^{-1}$ ,  $\mu_1 = 0.06 \text{ cm}^{-1}$  (no absorption correction), No. of measured reflections = 16 382, No. of unique = 3187,  $R_{\text{int}} = 0.016$ .

Neutron refinement:  $N_{\text{obs}} = 8867$  ( $I > 3\sigma(I)$ ),  $N_{\text{par}} = 708$ , GOF = 1.79,  $R_F = 0.082$ ,  $R_{\text{wF}} = 0.063$ .

Multipole refinement: The O, N, and C atoms were modeled with multipole expansions up to octupole level with two radial kappa parameters for each chemically unique type of atom (12 different kappa sets). The hydrogen atoms had multipole expansions to quadrupole level with positions and anisotropic thermal parameters fixed at values from the neutron refinement. The accuracy of the model can be tested by comparing thermal parameters for the heavy atoms derived separately from the X-ray and neutron data.<sup>[12]</sup> In the present case we obtain  $\langle \Delta U_{\text{X-N}} \rangle = 0.0009 \text{ \AA}^2$  and  $\langle U_{\text{X}}/U_{\text{N}} \rangle = 1.05$ . This demonstrates that the systematic errors are minimal,

and thus we can have confidence in the static model charge densities.  $N_{\text{obs}} = 11182$  (only multiple measured reflections),  $N_{\text{par}} = 1128$ ,  $\text{GOF} = 1.13$ ,  $R_{\text{F2}} = 0.035$ ,  $R_{\text{wF2}} = 0.046$ .

Received: December 14, 1998 [Z 127781E]  
German version: *Angew. Chem.* **1999**, *111*, 1321–1324

**Keywords:** charge density • enzyme catalysis • hydrogen bonds • neutron diffraction • serine proteases

- [1] D. M. Blow, J. J. Birktoft, B. S. Hartley, *Nature* **1969**, *211*, 337–340.
- [2] a) W. W. Cleland, M. M. Krevoy, *Science* **1994**, *264*, 1887–1890; b) P. A. Frey, S. A. Whitt, J. B. Tobin, *Science* **1994**, *264*, 1927–1935
- [3] A. Warshal, A. Papazyan, P. A. Kollman, *Science* **1995**, *269*, 102–104.
- [4] a) M. Garcia-Viloca, A. Gonzalez-Lafont, J. M. Lluch, *J. Am. Chem. Soc.* **1997**, *119*, 1081–1086; b) G. A. Kumar, M. A. McAllister, *J. Am. Chem. Soc.* **1998**, *120*, 3159–3165; c) B. Schiøtt, B. B. Iversen, G. H. K. Madsen, T. C. Bruice, *J. Am. Chem. Soc.* **1998**, *120*, 12117.
- [5] a) G. Gilli, F. Bellucci, V. Ferretti, V. Bertolasi, *J. Am. Chem. Soc.* **1989**, *111*, 1023–1028; b) T. Steiner, *J. Phys. Chem. A* **1998**, *102*, 7041–7052.
- [6] F. Hibbert, J. Emsley, *J. Adv. Phys. Org. Chem.* **1990**, *26*, 255–379.
- [7] a) E. D. Stevens, M. S. Lehmann, P. Coppens, *J. Am. Chem. Soc.* **1977**, *99*, 2829–2831; b) G. K. H. Madsen, B. B. Iversen, F. K. Larsen, M. Kapon, G. M. Reisner, F. H. Herbststein, *J. Am. Chem. Soc.* **1998**, *120*, 10040–10045.
- [8] R. F. W. Bader, *Atoms in molecules. A quantum theory*, Oxford University Press, Oxford, **1990**.
- [9] A. J. Schultz, K. Srinivasan, R. G. Teller, J. M. Williams, C. M. Lukehart, *J. Am. Chem. Soc.* **1984**, *106*, 999–1003.
- [10] a) N. K. Hansen, P. Coppens, *Acta Crystallogr. Sect. A* **1978**, *34*, 909–921; b) T. Koritsanszky, S. T. Howard, P. R. Mallinson, Z. Su, T. Richter, N. K. Hansen, Program XD, a computer program package for multipole refinement and analysis of charge densities from diffraction data **1995**, Institute of Crystallography, Freie Universität, Berlin, Germany.
- [11] E. Espinosa, E. Molins, C. Lecomte, *Chem. Phys. Lett.* **1998**, *285*, 170–173.
- [12] B. B. Iversen, F. K. Larsen, B. N. Figgis, P. A. Reynolds, A. J. Schultz, *Acta Crystallogr. Sect. B* **1996**, *52*, 923–931.

## Pentamethylcyclopentadienylrhodium(III) and -iridium(III) Complexes Showing P,O Coordination: Unprecedented Insertion of tcne and tcnq into a C–H Bond\*\*

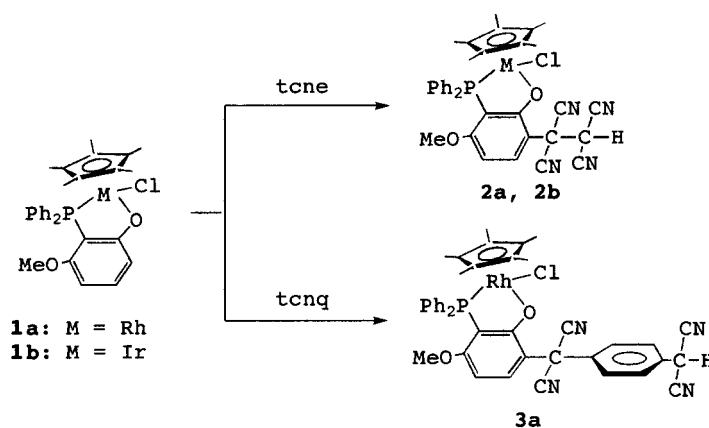
Yasuhiro Yamamoto,\* Xiao-Hong Han, Ken-ichiro Sugawara, and Saho Nishimura

Tetracyanoethylene (tcne) forms a variety of charge transfer and organometallic complexes as a result of its strong electrophilicity.<sup>[1]</sup> It is widely used as a precursor of organic

magnets, the tetracyanoethylene-based organic magnets.<sup>[2]</sup> Reactions of tcne with metal–acetylide, metal–hydride, or metal– $\eta^1$ -dienyl complexes exhibit characteristic features: 1) insertion into M–C bonds<sup>[3a, b]</sup> and into M–H bonds to afford cyano(dicyanomethyl)keteniminato complexes;<sup>[3c–e]</sup> 2) [2+2] addition to acetylide groups to give cyclobutene–metal complexes;<sup>[4]</sup> 3) [4+2] or [3+2] addition to diene moieties to produce cyclohexene– or cyclopentane–metal complexes;<sup>[5]</sup> 4)  $\alpha,\beta$  addition of dicyanomethylene fragments, derived from cleavage of the double bond of tcne, to an acetylide group.<sup>[6]</sup> In all cases except for (1), tcne is reactive to strongly activated unsaturated groups on the ligands.

Recently we reported that one of the *ortho*-methoxy groups in (2,6-dimethoxyphenyl)diphenylphosphane (MDMPP) is demethylated upon reaction with bis[dichloro( $\eta^6$ -arene)rhodium(III)] or bis[dichloro( $\eta^5$ -pentamethylcyclopentadienyl)rhodium(III)] to give  $[(\eta^6\text{-arene})\text{RuCl}(\text{MDMPP-}P,O)]^{[7a, b]}$  and  $[(\eta^5\text{-C}_5\text{Me}_5)\text{RhCl}(\text{MDMPP-}P,O)]^{[8]}$  respectively (MDMPP- $P,O$  =  $\text{PPh}_2(2\text{-O-6-MeO-C}_6\text{H}_3)$ , a P,O chelating phosphane). These complexes react with Lewis bases (L) in the presence of  $\text{PF}_6^-$  to give the corresponding cationic complexes  $[(\eta^6\text{-arene})\text{Ru}(\text{MDMPP-}P,O)(\text{L})][\text{PF}_6]^{[7c]}$  and  $[(\eta^5\text{-C}_5\text{Me}_5)\text{Rh}(\text{MDMPP-}P,O)(\text{L})][\text{PF}_6]^{[8]}$ . While investigating the interactions of these complexes with small molecules such as olefins and alkynes, we found that tcne inserted into a weakly activated C–H bond on the substituted phenyl ring of the phosphane ligand upon reaction with the rhodium(III) or iridium(III) complexes  $[(\eta^5\text{-C}_5\text{Me}_5)\text{MCl}(\text{MDMPP-}P,O)]$  (**1a**:  $\text{M} = \text{Rh}$ ,<sup>[8]</sup> **1b**:  $\text{M} = \text{Ir}$ <sup>[9]</sup>). This represents novel reactivity for tcne.

When tcne was added to **1a** or **1b** in  $\text{CH}_2\text{Cl}_2$  at room temperature (Scheme 1), the solution became brown or yellow. In each case a 1:1 adduct was isolated, which on the



Scheme 1. Reactions of complexes **1** with tcne or tcnq.

basis of fast atom bombardment (FAB) mass spectrometry was assigned as **2a** ( $m/z$  709 [ $M^+$ ], orange-brown) or **2b** ( $m/z$  798 [ $M^+$ ], yellow; see the Experimental Section). In the IR spectrum of **2a** a very weak  $\text{C}\equiv\text{N}$  stretching frequency appeared at  $2250\text{ cm}^{-1}$ , which is at higher energy than that of free tcne ( $2207\text{ cm}^{-1}$ ) and  $\pi$ -complexed tcne ( $2170\text{--}2235\text{ cm}^{-1}$ ).<sup>[1]</sup> However, no IR signal was observed for **2b** as bands in the  $\nu_{\text{CN}}$  region are extremely weak. In the  $^1\text{H}$  NMR spectra of **2** three characteristic resonances around  $\delta = 1.50$ ,

[\*] Prof. Dr. Y. Yamamoto, X.-H. Han, K. Sugawara, S. Nishimura  
Department of Chemistry, Faculty of Science  
Toho University  
Miyama, Funabashi, Chiba, 274–8510 (Japan)  
Fax: (+81) 474-75-1855  
E-mail: yamamoto@chem.sci.toho-u.ac.jp

[\*\*] We thank Professor Shigetoshi Takahashi and Ms. Fumie Takei at The Institute of Scientific and Industrial Research, Osaka University for measurement of FAB mass spectra.